Topographic Effects in Probabilistic Seismic Hazard Analysis: The Case of Narni, Central Italy

S. Barani
University of Genoa, Italy; GEAmb S.r.l. (Academic Spin-off Company), Genoa, Italy.

M. Massa & S. Lovati
Istituto Nazionale di Geofisica e Vulcanologia, Sezione Milano-Pavia, Italy

G. Ferretti
University of Genoa, Italy

SUMMARY:
This study presents a probabilistic method for estimating the ground motion hazard at sites presenting topographic irregularities. This method is applicable to topographic crests or ridges which may affect site response, producing 2D (or 3D) amplification effects. The method is based on a set of 2D numerical analyses that are carried out using multiple accelerograms from worldwide weak and strong earthquakes recorded on rock. Numerical analyses are performed to compute site-specific frequency-dependent amplification factors to be included into the ground motion prediction equation used in the seismic hazard computation. The hazard at the top of the ridge is then assessed by running a conventional probabilistic seismic hazard analysis (PSHA) with the attenuation relationship modified to include the site response. An application to the case study of Narni (Central Italy) is presented in this work.

Keywords: Probabilistic seismic hazard analysis, topographic effects, ground response analysis

1. INTRODUCTION

The term "Probabilistic Seismic Hazard Analysis" (PSHA) is commonly used to indicate the assessment of the probability that given ground motion levels on rock can be exceeded at a site characterized by a flat topography during a given period of time. However, it has long been recognized that geomorphology (e.g., topographic irregularities, alluvial valleys) as well as soil characteristics may have a strong impact on the level of ground motion induced by an earthquake at a site. Therefore, contrary to large-scale seismic hazard mapping, site-specific assessments should allow for amplification effects related to particular geological characteristics.

Bazzurro and Cornell (2004a and 2004b) recently developed a method that incorporates the amplification of nonlinear soil deposits into the framework of site-specific PSHA. Specifically, the method consists of convolving the hazard curve at the bedrock level with the probability distribution of the amplification function obtained after several numerical ground response analyses based on different input motions. A similar approach has been proposed by Barani et al. (2010) for estimating the earthquake-induced slope displacement via a probabilistic method. Again, the empirical soil response function, which is derived from regression of displacement values versus various alternative ground motion parameters (e.g., spectral acceleration, Housner intensity, Arias intensity), can be coupled with PSHA at the bedrock to establish the annual rate of exceedance of permanent slope deformation of different severity (Bazzurro et al., 1994; Rathje and Saygili, 2008).

The method presented in this article is an extension of the original approach of Bazzurro and Cornell (2004a and 2004b) for 1D site amplification assessment. Specifically, we present a probabilistic method for estimating the ground motion hazard at sites located in areas where local geomorphology may be responsible for complex bi- or tri-dimensional (2D or 3D) amplification effects. In particular, the method presented here is applicable to rocky crests or ridges which may affect site response, producing 2D (or 3D) linear amplification effects. Comprehensive studies and reviews concerning the

effects of surface topography on earthquake ground shaking can be found in articles of Davis and West (1973), Geli et al. (1988), Bard and Riepl-Thomas (1999), Paolucci (2002), Bouckovalas and Papadimitriou (2005).

As its predecessors, the method presented here consists of two steps. First, numerical ground response analyses are performed to estimate frequency-dependent amplification factors and their uncertainty. Then, a conventional PSHA is run by using a rock ground motion prediction equation (GMPE) modified to include site response. Differently to the original method of Bazzurro and Cornell (2004b), convolution is not necessary here as rocky ridges behave as perfect linear bodies.

The method is applied to the case study of Narni (Central Italy), a small village developed along the main axis of a rocky ridge. This site is chosen as it was extensively studied by Massa et al. (2010) using different experimental techniques based on spectral ratio measurements. Results from that study evidence the presence of directional amplification effects at frequencies between 4 and 5Hz (details are given in the next section) which may be related to surface topography.

Following a brief description of the study site, the article will deal with the definition of the ridge model used in the numerical simulations. Then, the ground response assessment will be presented and numerical amplification functions will be compared and contrasted with those obtained from experimental measurements by Massa et al. (2010). Finally, the site-specific seismic hazard method will be described and the hazard values resulting from its application will be compared with conventional estimates based on the assumption of flat topography.

2. DESCRIPTION OF SITE

Narni is a small village that was built along the main axis of a topographic ridge in the Central Apennines. The ridge, whose longitudinal length is approximately 1300m, is characterized by a steepness asymmetry, with a pronounced slope (≈ 35°) on the western side and a gentler slope (≈ 22°) on the eastern one (Figure 2.1.). Concerning geology, the ridge is characterized by a limestone massif composed of cherty and marly limestones interleaved with thin marly and clayed levels (Figure 2.2.).

Figure 2.1. View of the Narni ridge.

The ridge originated during the compressive geodynamic stage affecting the Central Apennines in the Miocene and Pliocene periods. Such tectonic deformations created normal and overturned folds, reverse faults and thrusts dipping towards the south and west. From the Pleistocene, a new extensional phase generated normal high-angle faults with southwestward and northeastward dip (Pierantoni, 1995). Despite this complex evolution, the level of fracturing characterizing the limestone massif is

negligible, particularly at the top of the ridge. Therefore, as regards the geomechanical setting, the ridge can be considered as a homogeneous body (Massa et al., 2010). Also concerning lithology, the ridge can be assumed as a single homogeneous block, although minor inhomogeneities and limestones of different age and composition are present (Figure 2.2.). Due to the complex tectonic processes mentioned above, limestones are arranged following a reverse stratigraphic order, with elder rocks at the top of the stratigraphy.

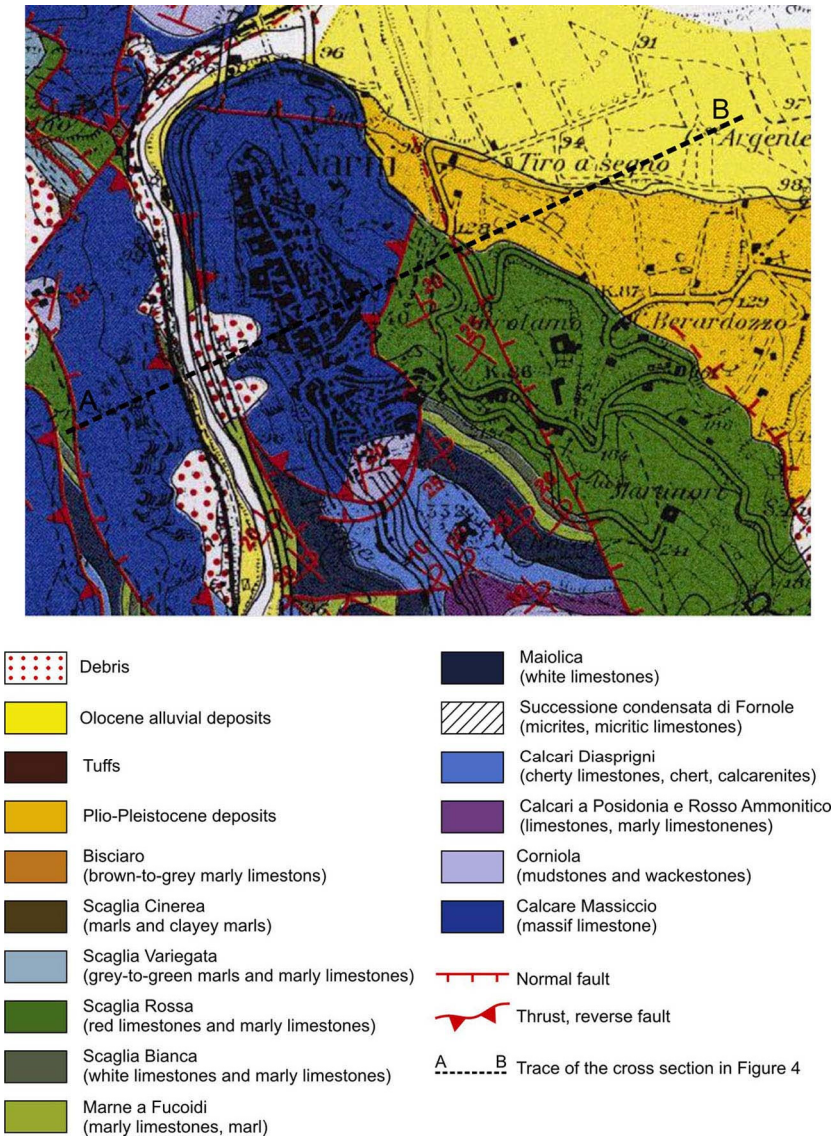

Figure 2.2. Geologic map (after Boncio et al., 2000)

Recently, the ground response of the Narni ridge has been exhaustively investigated by Massa et al. (2010) via experimental spectral ratio measurements. More specifically, a temporary seismic network of 10 stations, operating from March to September 2009, was installed both at the base and along the crest of the ridge. During that period, 702 earthquakes were recorded, including a large number (more than 600) of aftershocks belonging to the destructive 2009 L'Aquila sequence. Data were analyzed using both reference and non-reference site methods (these latter are often refer to as Horizontal to Vertical Spectral Ratio, HVSR, methods). Analyzing spectral ratios of earthquake recordings have revealed the presence of marked amplification effects for frequencies between 4 and 5Hz (Figure 2.3.). The largest amplifications were found for directions of the ground motion perpendicular to the main elongation of the ridge (i.e., for directions comprised between 60° and 100° as indicated by the green and light blues curves in Figure 2.3.). Mild amplification effects were also observed between 1 and 2Hz (Massa et al., 2010).

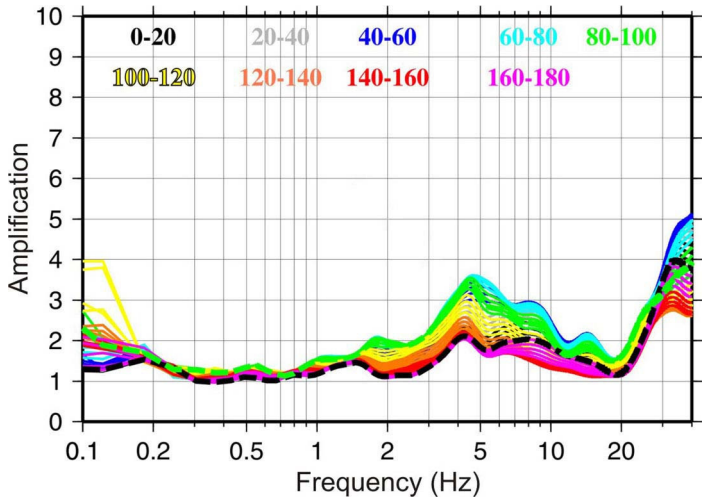

Figure 2.3. Standard spectral ratios for a site at the top of the Narni ridge (after Massa et al., 2010). Curves corresponding to different azimuth ranges (indicated on top of the figure) are indicated by different colours

3. NUMERICAL MODELLING AND GROUND RESPONSE ANALYSIS

In order to evaluate site amplification, 2D dynamic analyses were performed using the finite-element computer code QUAD4M (Hudson et al., 1994), which solves the dynamic response problem using an equivalent-linear, time-domain method. This program improves the original QUAD4 code (Idriss et al., 1973), which was modified to implement a transmitting base to minimize the artificial reflection of seismic waves from the half space underlying the finite element mesh.

The 2D model (Figure 3.1.) consists of approximately 9400 elements designed with consideration to the shear wave velocity characterizing the ridge, which was modelled as a homogeneous geologic medium with unit weight γ = 22kN/m^3, S-wave velocity V_S = 1400m/s, P-wave velocity V_P = 2500m/s, and shear modulus G_{max} = 4.3E+09Pa. Specifically, the criterion proposed by Kuhlemeyer and Lysmer (1973) was applied to establish the maximum element size compatible with accurate modelling of wave propagation through the medium, and elements smaller than approximately 1/10 to 1/8 of the wavelength associated with the highest frequency to be modelled were selected. A maximum element size of approximately 15m was adopted. According to this approach the model allows effective wave propagation up to around 9-12Hz.

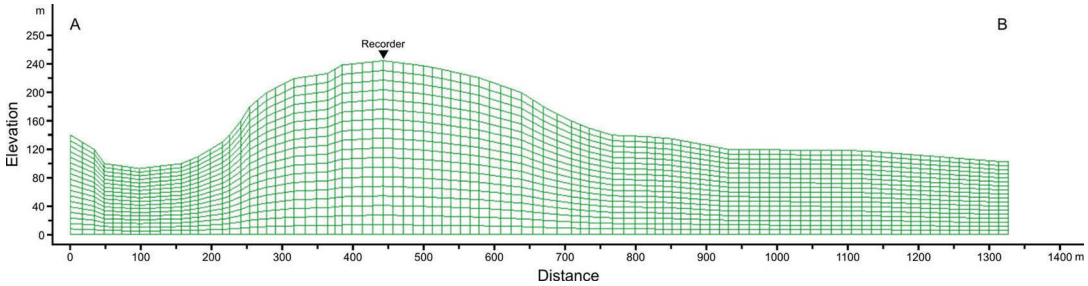

Figure 3.1. Numerical model used in the ground response analysis

The seismic input applied along the base of the model consists of a set of 35 real acceleration time histories from worldwide weak and strong earthquakes (note that the data set includes 29 Italian events) recorded at sites classified as “rock” (Table 3.1.). Here, the term “rock” refers to sites with average shear wave velocity in the upper 30m ($V_{S,30}$) greater than 800m/s, in accordance with the classification proposed by the Eurocode 8 (Comitè Europèen de Normalisation – CEN, 2003) and by the Italian building code (Ministero delle Infrastrutture e dei Trasporti, 2008). All records are consistent with the seismotectonic setting of the investigated area (where normal and strike-slip

mechanisms prevail) and with results obtained from the 2D disaggregation of the 0.2s (Figure 3.2.) and 1.0s (the disaggregation plot for this spectral period is not reported for brevity) spectral acceleration hazard corresponding to a mean return period (MRP) of 475 years. Records are selected in order to cover a wide range of PGA values (0.006g – 0.36g) compatible with the site PGA hazard, thus allowing the influence of both strong and weak motions on ground response results to be effectively evaluated. For each event, both the horizontal component with the highest peak ground acceleration (PHA) value and the vertical component were applied at the base of the model.

Table 3.1. List of ground motion records used in numerical simulations. M_w is for moment magnitude, M_s for surface wave magnitude R for epicentral distance, and PHA and PVA indicate peak horizontal and vertical acceleration, respectively

Earthquake Name	Country	Date	Latitude	Longitude	M_s	M_w	R (km)	Station Code	PHA (g)	PVA (g)	Databank
San Fernando	California	09/02/1971	34.44	-118.41	6.6	6.6	24.2	L04	0.1923	0.1635	PEER-NGA
Friuli	Italy	06/05/1976	46.29	13.25	6.5	6.5	23.0	TLM1	0.3567	0.2674	ESD
Friuli	Italy	11/09/1976	46.29	13.18	5.5	5.1	9.1	TRC	0.2432	0.0534	ITACA
Friuli	Italy	16/09/1977	46.28	12.98	5.1	5.3	9.1	SMU	0.1836	0.0566	ITACA
Patti Gulf	Italy	15/04/1978	38.268	15.112	5.8	6.0	33.0	NAS	0.1481	0.0811	ITACA
Valnerina	Italy	19/09/1979	42.8	13.04	5.9	5.8	50.1	SVT	0.0176	0.0093	ITACA
Irpinia	Italy	23/11/1980	40.76	15.309	6.8	6.9	78.3	TDG	0.0599	0.0340	ITACA
Friuli	Italy	01/02/1988	46.3595	13.0745	4.3	4.6	7.6	TLB	0.0063	0.0106	ITACA
Loma Prieta	California	18/10/1989	37.04	-121.88	6.9	6.9	96.3	PHT	0.0609	0.0306	PEER-NGA
Northridge	California	17/01/1994	34.21	-118.55	6.7	6.7	64.0	ATB	0.0683	0.0291	PEER-NGA
Northridge	California	17/01/1994	34.21	-118.55	6.7	6.7	45.8	MTW	0.2339	0.0870	PEER-NGA
Kozani	Greece	13/05/1995	40.18	21.66	6.5	6.5	71.0	FLO	0.0261	0.0188	ESD
Gargano	Italy	03/09/1995	41.8135	15.9143	5.2	5.2	28.5	SNN	0.1147	0.0345	ITACA
Umbria-Marche 1st Shock	Italy	26/09/1997	43.0228	12.891	5.6	5.7	24.3	MNF	0.0249	0.0178	ITACA
Umbria-Marche 1st Shock	Italy	26/09/1997	43.0228	12.891	5.6	5.7	35.2	CSC	0.0279	0.0160	ITACA
Umbria-Marche 2nd Shock	Italy	26/09/1997	43.0147	12.8538	6.1	6.0	27.5	MNF	0.0318	0.0206	ITACA
Umbria-Marche 2nd Shock	Italy	26/09/1997	43.0147	12.8538	6.1	6.0	60.6	CGL	0.0200	0.0184	ITACA
Umbria-Marche 2nd Shock	Italy	26/09/1997	43.0147	12.8538	6.1	6.0	43.2	GBB	0.0833	0.0318	ITACA
Umbria-Marche 2nd Shock	Italy	26/09/1997	43.0147	12.8538	6.1	6.0	21.4	ASS	0.1880	0.0765	ITACA
Umbria-Marche (aftershock)	Italy	03/10/1997	43.00	12.84	4.9	5.3	8.0	NCB	0.2838	0.0622	ESD
Appennino Umbro-Marchigiano	Italy	06/10/1997	43.0275	12.8467	5.1	5.4	14.1	NCM	0.1751	0.0711	ITACA
Umbria-Marche (aftershock)	Italy	06/10/1997	43.02	12.84	5.2	5.5	10.0	NCB	0.3608	0.1189	ESD
Umbria-Marche 3rd Shock	Italy	14/10/1997	42.8982	12.8987	5.6	5.6	22.0	CSC	0.0633	0.0591	ITACA
Umbria Marche (aftershock)	Italy	14/10/1997	42.92	12.93	5.6	5.6	12.0	CTR	0.3366	0.1603	ESD
Appennino Umbro-Marchigiano	Italy	09/11/1997	42.8462	12.9882	4.9	4.8	14.3	CSC	0.0134	0.0084	ITACA
Appennino Umbro-Marchigiano	Italy	03/04/1998	43.1853	12.7568	4.7	5.1	5.2	NCM	0.1280	0.0865	ITACA
Chi-Chi	Taiwan	25/09/1999	23.87	121.01	6.3	6.3	66.2	HWA003	0.0379	0.0134	PEER-NGA
L'Aquila Mainshock	Italy	06/04/2009	42.334	13.334	6.3	6.3	88.5	CDS	0.0101	0.0071	ITACA
L'Aquila Mainshock	Italy	06/04/2009	42.334	13.334	6.3	6.3	49.3	ORC	0.0653	0.0311	ITACA
L'Aquila Mainshock	Italy	06/04/2009	42.334	13.334	6.3	6.3	31.6	CLN	0.0902	0.0448	ITACA
L'Aquila Mainshock	Italy	06/04/2009	42.366	13.34	4.7	5.1	1.6	AQM	0.3387	0.0990	ITACA
L'Aquila	Italy	07/04/2009	42.342	13.338	4.5	5.0	5.3	AQP	0.0379	0.0181	ITACA
L'Aquila	Italy	07/04/2009	42.275	13.464	5.4	5.6	14.4	AQP	0.0940	0.0431	ITACA
L'Aquila	Italy	07/04/2009	42.275	13.464	5.4	5.6	10.0	MI01	0.2296	0.0737	ITACA
L'Aquila	Italy	07/04/2009	42.38	13.376	4.0	4.6	0.7	AQP	0.1696	0.1055	ITACA

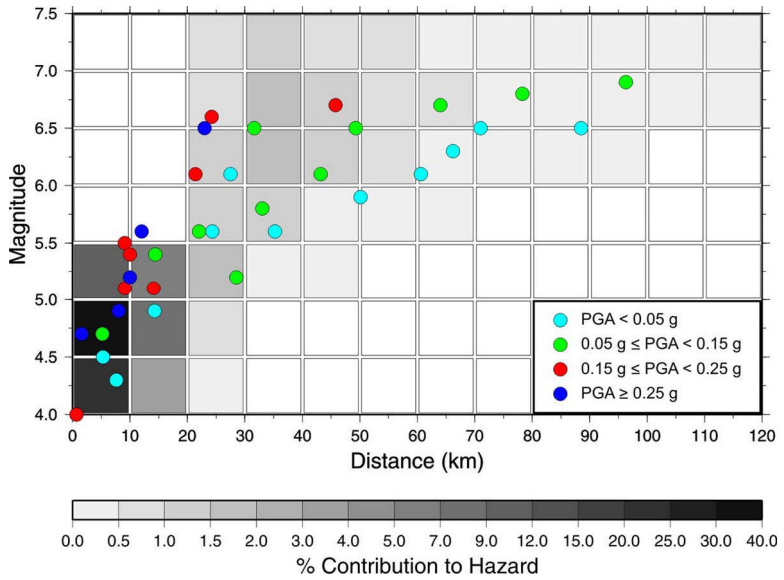

Figure 3.2. Contributions to the 0.2s spectral acceleration hazard for an MRP of 475 years

The amplification functions, *AF*(*f*), resulting from the ground response analysis are shown in Figure 3.3. Each *AF*(*f*) is defined as the Fourier spectral ratio of the ground motion recorded at the top and base of the ridge. Note that the topographic cross section (Figure 3.1.) was extended on both sides to avoid recording of reflected waves propagating back into the grid. Indeed, contrary to other computer programs, QUAD4M does not allow for absorbing boundaries on the model sides. The recorder at the base of the ridge was located at approximately 2.5km from both the left side of the model and the foot of the relief.

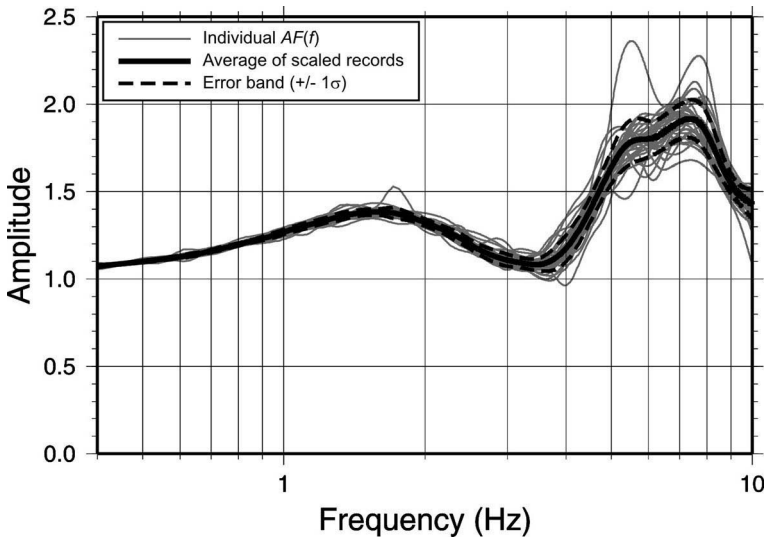

Figure 3.3. Numerical amplification functions

Analyzing the amplification functions in Figure 3.3. evidences two amplification peaks, at approximately 1.6Hz and between 5Hz and 8Hz. Both peaks agree well with those obtained from earthquake recordings (Figure 2.3.), particularly that at 1.6Hz which replicates faithfully the actual amplification determined from spectral ratio measurements. The second peak, instead, slightly underestimates the amplification level derived from experimental measurements. This may be associated to oversimplification of the numerical model or to analytical solutions, which may be ineffective in reproducing the complex modifications that a wave field undergoes in the proximity of a steep topography.

4. SEISMIC HAZARD ANALYSIS: METHOD AND RESULTS

Contrary to site-specific applications including the nonlinear soil response (Bazzurro and Cornell, 2004a and 2004b), the case study presented here does not require the estimation of a specific response function (i.e., a function that predicts site amplification as a function of one or more ground motion parameters or earthquake characteristics) to be convolved with the rock-outcrop hazard. Indeed, as shown in Figure 4.1., the ground motion amplification at the top of a rocky ridge does not vary with earthquake magnitude and distance or as a function of the input motion level (Figure 4.1). Therefore, the site amplification can be directly included into an existing rock GMPE for $S_a(f)$ (see also the article of Bazzurro and Cornell (2004b)):

$$\log S_a^{crest}(f) = \log S_a(f) + \log AF(f) \tag{4.1}$$

$$\log S_a^{crest}(f) = \log \overline{S_a(f)} + \varepsilon_{\log S_a(f)}\sigma_{\log S_a(f)} + \log \overline{AF(f)} + \varepsilon_{\log AF(f)}\sigma_{\log AF(f)} \tag{4.2}$$

where $S_a^{crest}(f)$ is the spectral acceleration at the crest of the ridge, $\log \overline{S_a(f)}$ is the median of $\log S_a(f)$ predicted by a GMPE given M and R (and, possibly, other characteristics that are

commonly taken into account in modern attenuation relations, such as the source mechanism), $\log \overline{AF(f)}$ is the median of $\log AF(f)$, $\varepsilon_{\log S_a(f)}$ and $\varepsilon_{\log AF(f)}$ are standard normal variables, and $\sigma_{\log S_a(f)}$ and $\sigma_{\log AF(f)}$ are the standard errors of $\log S_a(f)$ and $\log AF(f)$ respectively.

The dispersion measure for log(S_a) at the crest of the ridge becomes (Table 4.1.):

$$\sigma_{\log S_a^{crest}(f)} = \sqrt{\sigma^2_{\log S_a(f)} + \sigma^2_{\log AF(f)}} \tag{4.3}$$

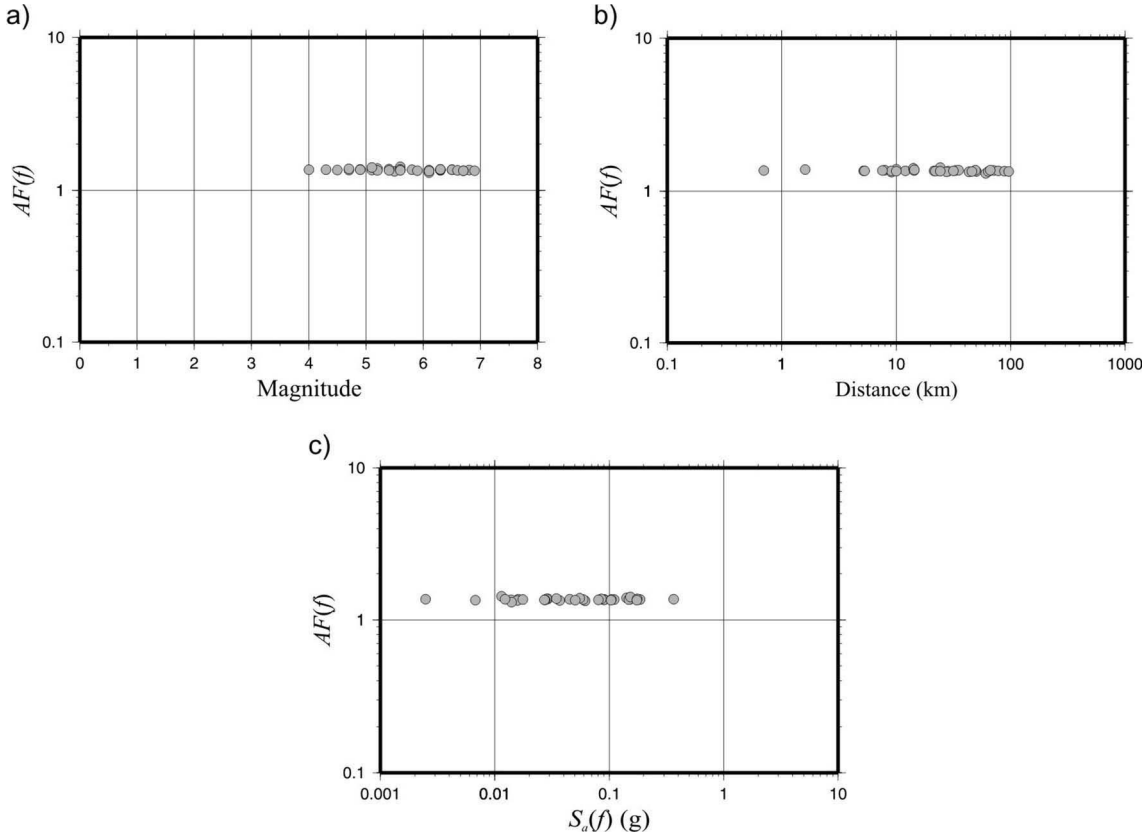

Figure 4.1. Variation of $AF(f = 1.67\text{Hz})$ as a function of (a) magnitude, (b) epicentral distance, and (c) 1.67Hz spectral acceleration

The hazard at the base of the ridge was calculated using the standard source-based approach originally proposed by Cornell (1968) and subsequently improved by many others. Input parameters and models are those used for the seismic hazard assessment of Italy (Gruppo di Lavoro MPS, 2004) with the exception of the ground motion attenuation relation. In this application, the GMPE of Bindi et al. (2009), which was calibrated based on Italian strong motion data (Working Group ITACA, 2010), was used. Note that this attenuation equation was developed for the larger of the two horizontal components. Therefore, according to Barani et al. (2010), all acceleration time histories used in the numerical simulations were selected compatibly with the definition of the GMPE used in the PSHA.

Figure 4.2. compares the uniform hazard spectra (UHS) calculated at the base and top of the Narni ridge for three different MRPs: 475, 975, and 2475 years. As evident from the figure, neglecting site amplification produced by local topographic conditions may result in severe hazard underestimation, particularly in the frequency range where larger amplifications are observed. Indeed, for all three MRPs considered, the 0.15s spectral acceleration at the top of the ridge is almost twice that at the base. For instance, for an MRP of 475 years, the 0.15s spectral acceleration calculated using the standard approach (≈ 0.37g) and that obtained from the site-specific method (≈ 0.70g) differ by more than 85%.

Table 4.1. Values of $\log \overline{AF(f)}$, $\sigma_{\log AF(f)}$, and $\sigma_{\log S_a(f)}$ at the base and top of the ridge

Period (s)	Frequency (Hz)	$\log \overline{AF(f)}$	$\sigma_{\log AF(f)}$	$\sigma_{\log S_a(f)}$	$\sigma_{\log S_a^{crest}(f)}$
0.00	100.00	0.152	0.057	0.356	0.360
0.03	33.33	-0.434	0.404	0.355	0.538
0.04	25.00	-0.097	0.196	0.368	0.417
0.07	14.29	-0.105	0.053	0.368	0.372
0.10	10.00	0.153	0.029	0.376	0.377
0.15	6.67	0.270	0.023	0.386	0.387
0.20	5.00	0.214	0.025	0.395	0.396
0.25	4.00	0.069	0.029	0.385	0.386
0.30	3.33	0.035	0.012	0.380	0.380
0.35	2.86	0.050	0.014	0.379	0.380
0.40	2.50	0.078	0.010	0.378	0.378
0.45	2.22	0.105	0.008	0.378	0.379
0.50	2.00	0.122	0.007	0.375	0.375
0.60	1.67	0.140	0.008	0.378	0.378
0.70	1.43	0.139	0.006	0.381	0.381
0.80	1.25	0.128	0.006	0.381	0.381
0.90	1.11	0.115	0.006	0.384	0.384
1.00	1.00	0.104	0.005	0.396	0.396
1.25	0.80	0.078	0.003	0.406	0.406
1.50	0.67	0.060	0.003	0.411	0.411
1.75	0.57	0.049	0.003	0.395	0.395
2.00	0.50	0.041	0.002	0.376	0.376

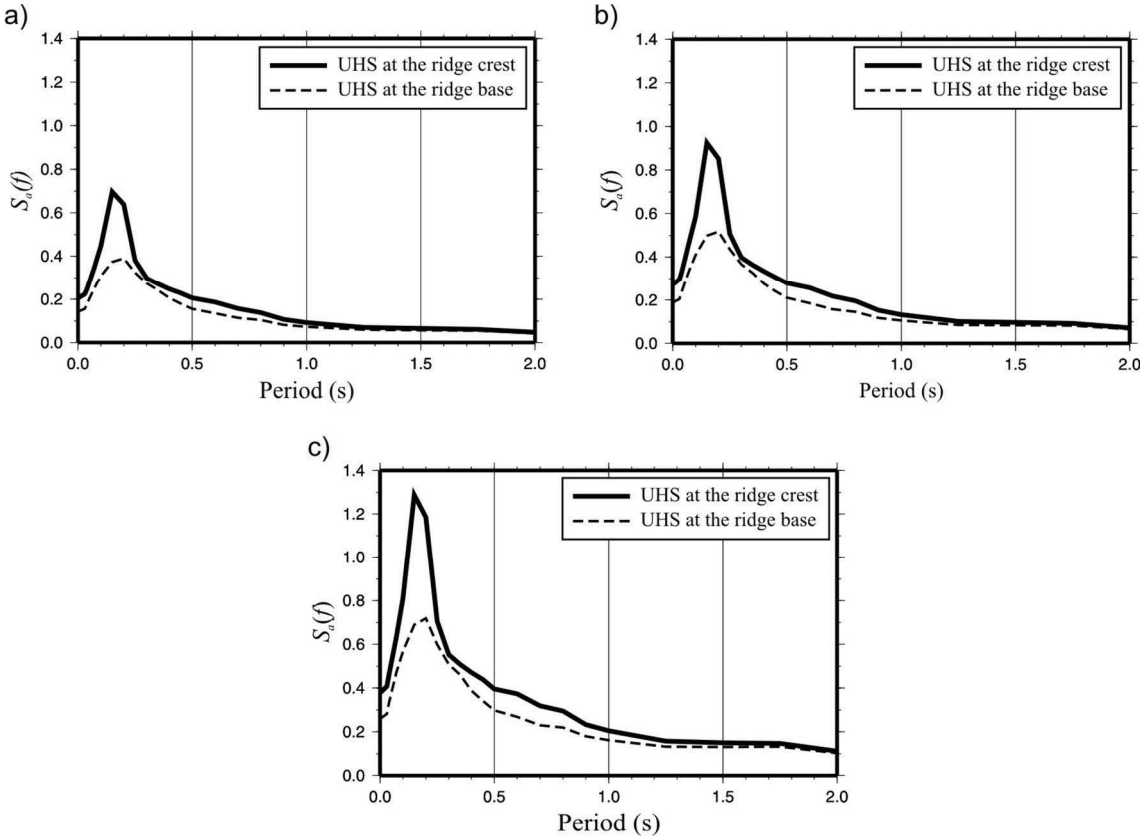

Figure 4.2. Uniform hazard spectra associated to MRPs of (a) 475, (b) 975, and (c) 2475 years

5. CONCLUSIONS

This study has presented a probabilistic method for estimating the ground motion hazard at rock sites affected by topographic irregularities or, more generally, at sites located in areas presenting complex geomorphology where 2D (or 3D) amplification effects may arise. The method could be also extended with some changes (i.e., a regression model predicting the soil amplification as a function of one or more rock ground motion parameters is required) to alluvial valleys where basin geometry and filling sediments concur in the definition of site response. In this case, the uncertainty affecting soils could be taken into account through Monte Carlo randomization (e.g., Bazzurro and Cornell, 2004a; Barani et al., 2008; Barani et al., 2012) with the disadvantage of blowing up the computation time. However, it is worth noting that the effect of the uncertainty in the soil parameters is of secondary importance compared to influence of the input motion variability (Bazzurro and Cornell, 2004a), at least in those cases when no significant impedance contrasts are present (Barani et al., 2012). In these cases, the input motion variability dominates the total uncertainty affecting ground response results and, consequently, the uncertainty in the soil model may be neglected. On the other hand, the effect of shear wave velocity becomes predominant when strong impedance contrasts exist (Barani et al., 2012).

The method proposed here consists of running multiple recordings (from strong and weak earthquakes) through a 2D numerical model of the investigated site. Empirical amplification factors are then computed and included into an existing rock GMPE, transforming it into a site-specific attenuation equation. In this application, 35 rock accelerograms were driven through the numerical model of the ridge under study. However, a sufficiently accurate estimate of the median $AF(f)$ can be obtained by using very few records (e.g., less than a dozen). Indeed, our results have shown that the resonance frequency of a topographic irregularity is rather insensitive to the amplitude and frequency content of the incoming motion.

Comparing site-specific hazard results with conventional estimates (i.e., that is assuming flat topography) has revealed that neglecting the site amplification produced by local topographic conditions may result in severe hazard underestimation. We found that, in the frequency range where larger amplifications are observed, the hazard near the crest of a ridge may be as large as twice that calculated assuming a flat topography. Therefore, conventional hazard estimates based on the assumption of flat topography may be very unconservative.

A final remark concerns the discrepancy between numerical and experimental ground response results. As observed previously, numerical amplification factors may underestimate the actual amplification level estimated through experimental measurements. The major reasons for this discrepancy may be found in the oversimplification of the numerical model or in possible limitations of analytical solutions. Such underestimation of the amplification level will be reflected in the hazard results. Hence, underestimating site amplification may result in unconservative hazard estimates, particularly in the frequency range around the site fundamental frequency. Therefore, future research will focus on the sensitivity of site-specific hazard estimates to model geometry and model parameterization.

AKCNOWLEDGEMENTS

We would like to acknowledge Regione Umbria and Floriana Pergalani (Politecnico di Milano) for providing us with geological and geotechnical data used in the numerical modelling.

REFERENCES

Barani, S., Bazzurro, P. and Pelli, F. (2010). A probabilistic method for the prediction of earthquake-induced slope displacements. *Fifth International Conference on Recent Advances in Geotechnical Earthquake Engineering and Soil Dynamics*. Paper No. 4.31b.

Barani, S., De Ferrari, R. and Ferretti, G. (2012). Influence of soil modeling uncertainties on site response. *Submitted to Earthquake Spectra*.

Barani, S., De Ferrari, R., Ferretti, G. and Eva, C. (2008). Influence of soil property uncertainties on ground

motion amplification. *31st Assembly of the European Seismological Commission*. 49-58.
Bard, P.-Y. and Riepl-Thomas, J. (1999). Wave propagation in complex geological structures and their effects on strong ground motion. In *Wave Motion in Earthquake Engineering*, Kausel, E. and Manolis G.D. (eds.), International Series on Advances in Earthquake Engineering, WIT Press, Southampton, Boston, 37-95.
Bazzurro, P. and Cornell, C.A. (2004a). Ground-motion amplification in nonlinear soil sites with uncertain properties. *Bulletin of the Seismological Society of America* **94:6**, 2090-2109.
Bazzurro, P. and Cornell, C.A. (2004b). Nonlinear soil-site effects in probabilistic seismic-hazard analysis. *Bulletin of the Seismological Society of America* **94:6**, 2110-2123.
Bazzurro, P., Pelli, F., Manfredini, G.M. and Cornell, C.A. (1994). Stability of sloping seabed: Seismic damage analysis: Methodology and application. *Third Symposium on Strait Crossings*. 821-829.
Bindi, D., Luzi, L., Massa, M. and Pacor, F. (2009). Horizontal and vertical ground motion prediction equations derived from the Italian Accelerometric Archive (ITACA). *Bulletin of Earthquake Engineering* **8:5**, 1209-1230.
Boncio, P., Brozzetti, F., Lavecchia, G., Bacheca, A. and Minelli, G. (2000). Note stratigrafiche e strutturali alla carta geologica del settore centrale della catena Narnese-Amerina (Umbria, scala 1:25000). *Bollettino della Società Geologica Italiana* **119**, 69-83.
Bouckovalas, G.D. and Papadimitriou, A.G. (2005). Numerical evaluation of slope topography effects on seismic ground motion. *Soil Dynamics and Earthquake Engineering* **25**, 547-558.
Comitè Europèen de Normalisation (2003). prENV 1998-1 – Eurocode 8: Design of structures for earthquake resistance. Part 1: General rules, seismic actions and rules for buildings. Draft No. 4, Brussels, Belgium.
Cornell, C. A. (1968). Engineering seismic risk analysis. *Bulletin of the Seismological Society of America* **58:5**, 1583-1606.
Davis, L.L. and West, L.R. (1973). Observed effects of topography on ground motion. *Bulletin of the Seismological Society of America* **63:1**, 283-298.
Geli, L., Bard, P.-Y. and Jullien, B. (1988). The effect of topography on earthquake ground motion: a review and new results. *Bulletin of the Seismological Society of America* **78:1**, 42-63.
Gruppo di Lavoro MPS (2004). Redazione della mappa di pericolosità sismica prevista dall'Ordinanza PCM 3274 del 20 marzo 2003, Rapporto conclusivo per il dipartimento di Protezione Civile. INGV, Milano – Roma, aprile 2004, 65 pp. + 5 appendici, http://zonesismiche.mi.ingv.it/elaborazioni/
Hudson, M., Idriss, I.M. and Beikae, M. (1994). QUAD4M, a computer program for evaluating the seismic response of soil structures using finite element procedures and incorporating a compliant base. Center for Geotechnical Modeling Department of Civil & Environmental Engineering, University of California, Davis.
Idriss, I.M., Lysmer, J., Hwang, R. and Seed, B.H. (1973). Quad4, a computer program for evaluating the seismic response of soil structures by variable damping finite element procedures. Report No. EERC 73-16, College of Engineering, University of California, Berkeley.
Kuhlemeyer, R.L. and Lysmer J. (1973). Finite element method accuracy for wave propagation problems. *Journal of Soil Mechanics and Foundations* **99:5**, 421–427.
Massa, M., Lovati, S., D'Alema, E., Ferretti, G. and Bakavoli, M. (2010). An experimental approach for estimating seismic amplification effects at the top of a ridge, and the implication for ground-motion predictions: the case of Narni, Central Italy. *Bulletin of the Seismological Society of America* **100:6**, 3020-3034.
Ministero delle Infrastrutture e dei Trasporti (2008). Norme tecniche per le costruzioni – NTC, D.M. 14 Gennaio 2008. Supplemento ordinario alla Gazzetta Ufficiale No 29, 4 Febbraio 2008.
Paolucci, R. (2002). Amplification of earthquake ground motion by steep topographic irregularities. *Earthquake Engineering and Structural Dynamics* **31**, 1831-1853.
Petrini, V., Pergalani, F. and Compagnoni, M. (2011). Microzonazione sismica Narni 1 + Narni 2 (Comune di Narni). Convenzione tra Regione dell'Umbria e Dipartimento di Ingegneria Strutturale Politecnico di Milano.
Pierantoni, P.P. (1995). Caratterizzazione geologico-strutturale dell'Appennino umbro-sabino: Monti Martani, dorsale narnese-amerina e Monti Sabini. PhD Thesis, University of Camerino.
Rathje, L.M. and Saygili, G. (2008). Probabilistic seismic hazard analysis for the sliding displacement of slopes: scalar and vector approaches. *Journal of Geotechnical and Geoenvironmental Engineering* **134:6**, 804-814.
Working Group ITACA (2010). Data Base of the Italian strong motion records. http://itaca.mi.ingv.it